Trends in

Applied Sciences Research

ISSN 1819-3579

Academic
Journals Inc.

www.academicjournals.com

Trends in Applied Sciences Research 6 (6): 595-605, 2011
ISSN 1819-3579 / DOI: 10.3923/tasr.2011.595.605

CFD Modeling of Heat and Mass Transfer in the Fluidized Bed Dryer

M. Keshavarz Moraveji, S.A. Kazemi and R. Davarnejad
Department of Chemical Engineering, Faculty of Engineering, Arak University, Arak 38156-8-8349, Iran

Corresponding Author: M. Keshavarz Moraveji, Department of Chemical Engineering, Faculty of Engineering, Arak University, Arak 38156-8-8349, Iran Tel: +98-9363098063 Fax: +98-861-4173450

ABSTRACT
Heat and mass transfer during drying process in a fluidized bed dryer have been modeled with Computational Fluid Dynamics (CFD) method. An Eulerian- Eulerian two fluid model incorporating kinetic theory was used for simulation of gas-solid flow. Governing equations were discretized based on finite volume in two-dimension and discretized algebraic equations were solved iteratively with Semi Implicit Method for Pressure Linked Equations (SIMPLE) method. The effects of operating conditions involving inlet gas velocity, inlet gas temperature, inlet solid temperature, initial solid moisture and particle size on the drying process were investigated. The modeled data were in good agreement with the experimental data obtained from the literature.

Key words: Two-fluid model, gas-solid flow, heat transfer, mass transfer, finite volume

INTRODUCTION
Recently various methods for drying process of solids have been developed. Thermal efficiency of the fluidized bed dryers is most important item for variety of drying applications (Mujumdar, 1995; Strumillo and Kudra, 1996). In this type of dryers, the drying gas in a boiling bed unit fluidizes the solids. Mixing and heat transfer processes are very rapid. The exit gas is usually saturated with vapor for any allowable fluidization velocity. These dryers may also be operated batch wise (Souraki and Mowla, 2008). There is interest in predicting the hydrodynamic behavior of fluidized beds.

While there are several experimental procedures for measuring heat and mass transfer phenomena in the fluidized bed, the use of CFD tools for providing valuable information for design of the reactor, scale up and optimization has attracted considerable attention in the recent years (Hekmat *et al*., 2010; Azizi *et al*., 2010). Two methods have been typically used for CFD modeling of gas-solid flows, namely, Eulerian-Lagrangian method and Eulerian-Eulerian approach. In the Eulerian-Lagrangian approach, the computational demand rises sharply with the number of traced particles, which constrains its applicability to high concentration flows. In the Eulerian-Eulerian method, which is used in the current study, two phases are mathematically treated as interpenetrating continua. The theoretical fundamental and equations for two-fluid method is explained in detail in the literature (Ishii, 1975; Gidaspow, 1994).

Researchers have conducted several numerical studies to describe fluidized bed drying process. Hoebink and Rietema (1980a) and Kerkhof (1994) presented some models based on temperature and humidity as homogeneous variables. Thomas and Varma (1992) showed a model which solid particles receded evaporation interface. The diffusive models were studied by Hoebink and Rietema (1980b), Zahed *et al*. (1995) and Van Ballegooijen *et al*. (1997). They considered the humidity profiles inside the particles. Palancz (1983) proposed a mathematical model for continuous fluidized bed drying based on the two-phase fluidization. According to this model, the fluidized bed was divided into two phases involving a bubble and an emulsion phase. An improvement in Palancz's model was carried out by Lai and Chen (1986). Garnavi *et al.* (2006) continued Palancz's work. They considered variation of bubble size along the bed height as well. Chandran *et al.* (1990) investigated single and spiral fluidized beds in a batch and continuous system. Tsotsas (1994) and Groenewold and Tsotsas (1997) modeled the heat and mass transfer in a batch fluidized bed using a normalized decreasing transfer rate related to the humidity of a single particle.

Hajidavalloo and Hamdullahpur (2000a, b) and proposed a mathematical model for heat and mass transfer simulation in a fluidized bed drying for large size particles. Wang and Chen (2000) studied bed dynamics in a fluidized bed as a perfect mixer without bubbles. Syahrul *et al.* (2002) were used mass, energy and entropy balances in a batch fluidized bed dryer by assuming perfect mixing of particles. Wildhagen *et al.* (2002) showed a three-phase model involving solid (as lumped), interstitial and bubble gas (as a perfect plug flow). Vitor *et al.* (2004) studied the effective heat and mass transfer coefficients estimated between interstitial gas and solid phases in drying process of biomass in a batch fluidized bed dryer. Burgschweiger and Tsotsas (2002) experimentally considered and theoretically modeled a continuous fluidized bed drying under steady state and dynamic conditions.

Izadifar and Mowla (2003) presented a model for a continuous fluidized bed dryer. According to this model, moisture content of particle and the latent heat of desortion vaporization were not constant values. Souraki *et al.* (2009) modeled the drying process of small spherical porous particles in a microwave fluidized bed dryer assisted with inert glass beads particles. Ishii (1975) used a two-fluid model for a packed bed dryer. Basirat-Tabrizi *et al.* (1983, 2002) extended Ishii’s model for a fluidized bed dryer. Basirat-Tabrizi *et al.* (1983) showed a model to simulate drying process for two-dimensional cylindrical cases.

In this study, CFD method was used for heat and mass transfer studying during drying process. The Eulerian-Eulerian two-fluid model was used to simulate the gas-solid flow. The modeling results are compared with the experimental data reported by Basirat-Tabrizi *et al.* (1983) and also compared with results from commercial CFD software (Fluent 6.3).

Computational fluid dynamic model: The conservation of mass and momentum and constitutive relations were studied elsewhere (Azizi *et al.*, 2010). Here, the heat and species conservation equations are briefly summarized.

Heat transfer modeling: Thermal energy equations for the gas phase are derived as following:

$$\varepsilon_g \rho_g C_{pg}\left(\frac{\partial}{\partial t}T_g + \vec{V}_g.\nabla T_g\right) = -\sum_{m=1}^{2}\left(H_{gm}\right) - \Delta H_{rg} \tag{1}$$

The thermal energy balance for the solid phases is given as:

$$\varepsilon_{sm}\rho_{sm}C_{psm}\left(\frac{\partial}{\partial t}T_{sm} + \vec{V}_{sm}.\nabla T_{sm}\right) = \nabla.\varepsilon_{sm}k_{sm} - H_{rsm} + H_{sm} \tag{2}$$

The heat transfer between the gas and the solids is a function of temperature difference between the gas and solid phases:

$$H_{gm} = -\gamma_{gm}\left(T_{sm} - T_g\right) \tag{3}$$

The heat transfer coefficient is related to the particle Nusselt number using the following equation:

$$\gamma_{gm} = \frac{C_{pg}R_{0m}}{e^{\left(C_{pg}R_{0m}/\gamma^0_{gm}\right)} - 1} \tag{4}$$

$$\gamma^0_{gm} = \frac{6k_g\varepsilon_{sm}Nu_m}{d^2_{pm}} \tag{5}$$

The Nusselt number is determined applying the following correlation (Gunn, for a porosity range of 0.35-1.0 and a Reynolds number up 10^5:

$$Nu_m = (7 - 10\varepsilon_g + 5\varepsilon_g^2)(1 + 0.7Re_m^{0.2}pr^{1/3}) + (1.33 - 2.4\varepsilon_g + 1.2\varepsilon_g^2)Re_m^{0.7}pr^{1/3} \tag{6}$$

Mass transfer modeling: In a complete mixing fluidized bed dryer, the surface moisture of the samples (at the end of drying process) will be assumed to be at equilibrium with the drying air. The species equation for the gas phase is:

$$\frac{\partial}{\partial T}\left(\varepsilon_g\rho_g X_g\right) + \nabla.\left(\varepsilon_g\rho_g X_g \overrightarrow{V_g}\right) = R_g \tag{7}$$

where, X_g is the mass fraction and R_g is the rate of formation of gas species (evaporation rate). The species equation for the solid phase is as the following:

$$\frac{\partial}{\partial T}\left(\varepsilon_{sm}\rho_{sm} X_{sm}\right) + \nabla.\left(\varepsilon_{sm}\rho_{sm} X_{sm} \overrightarrow{V_{sm}}\right) = R_{sm} \tag{8}$$

where, R_{sm} is the moisture evaporation from the particle surface.

Numerical simulation: The governing equations were discretized using finite volume method (the second-order upwind scheme) and discretized algebraic equations were solved iteratively with SIMPLE method (Ergun, 1952). The CFD open-source code MFIX is used for the present study (Azizi *et al*., 2010). The convergence criterion (for time zone) of 10^{-4} is specified for the relative error between successive iterations. The computational domain consists 35 grids in radial and 40 grids along the axis of the bed. So, the total grids will be around 1400. When the grids increase to 3000 (50×60) or decrease to 600 (20×30) the modeling results (velocity and temperature distributions) will not change significantly. Therefore, the obtained results in this range will be independent of meshes number. The initial bed of solids is packed into the bottom of the bed up to 0.6 m of bed height. The bottom of the bed is defined as inlet velocity to specify a uniform inlet gas velocity. Pressure boundary conditions were employed at the top of the freeboard which is set to a standard value of 1.0132×10^5 Pa.

RESULTS AND DISCUSSION

In the present study the Wheat grains was used as solid particles with initial temperature of 298 K, initial moisture content of 0.25 kg kg^{-1}, density of 1200 kg m^{-3} and diameter of 3 mm. The air enters the bed with initial moisture content of 0.015 kg kg^{-1}. The wall temperature was assumed to be in the adiabatic condition. Results of this simulation were obtained after 250 sec. The operating conditions effects such as the inlet gas velocity, inlet gas temperature, inlet solid temperature, initial solid moisture and particle size on the drying process were also investigated.

According to the Fig. 1 and 2, temperature and moisture content of solid profiles are in good agreement with the experimental data obtained by Basirat-Tabrizi *et al.* (1983). Figure 1-7 show the temperature and moisture content changes profile at various drying times. The required time

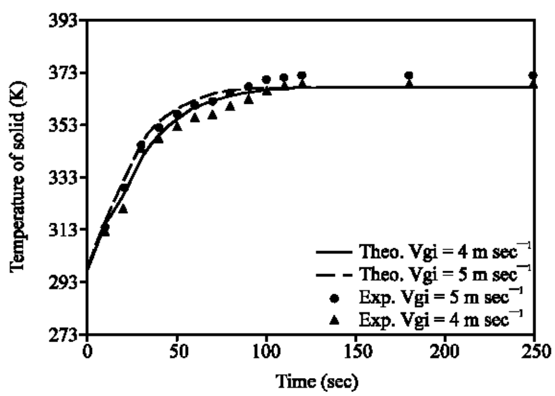

Fig. 1: Temperature of solid in fluidized bed at various gas velocities (4 and 5 m sec^{-1}) at temperature of 373 K

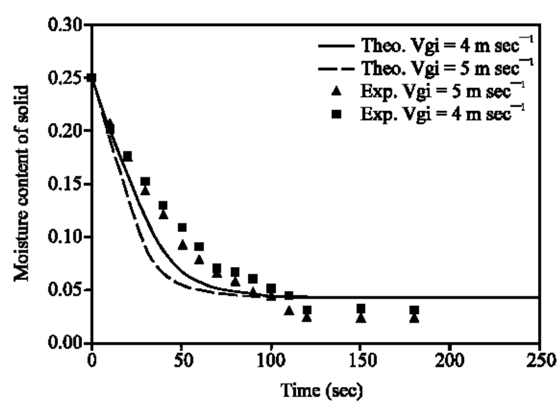

Fig. 2: Moisture content of solid in fluidized bed at various gas velocities (4 and 5 m sec^{-1}) at temperature of 373 K

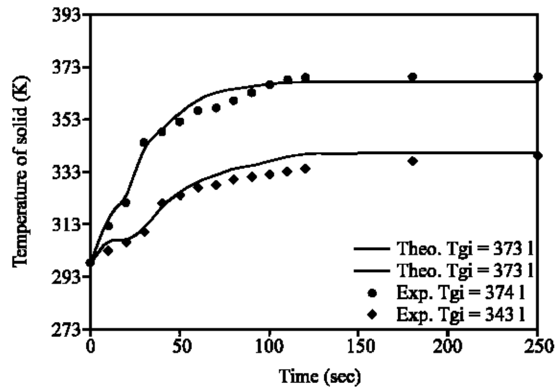

Fig. 3: Temperature of solid in fluidized bed at various gas temperatures (343 and 373 K) at velocity of 4 m sec^{-1}

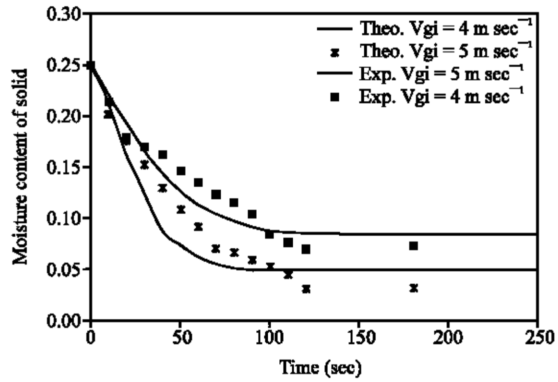

Fig. 4: Moisture content of solid in fluidized bed at various gas temperatures (343 and 373 K) at velocity of 4 m sec^{-1}

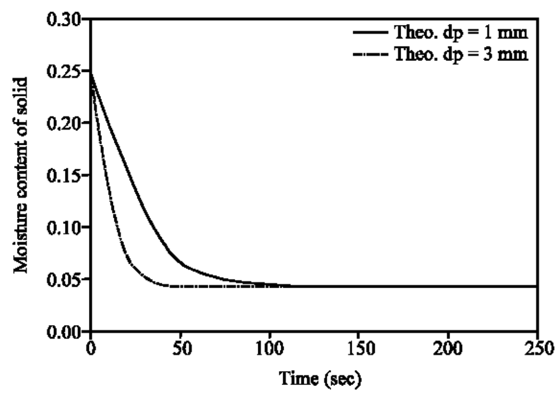

Fig. 5: Moisture content of solid in fluidized bed at various particle diameters (1 and 3 mm)

for moisture content and moisture content equilibrium will be obtained from moisture content versus time curve. Figure 1 and 2 show the effect of initial air velocity on drying process at gas temperature of 373 K. The profiles of temperature and moisture content of solid show that these

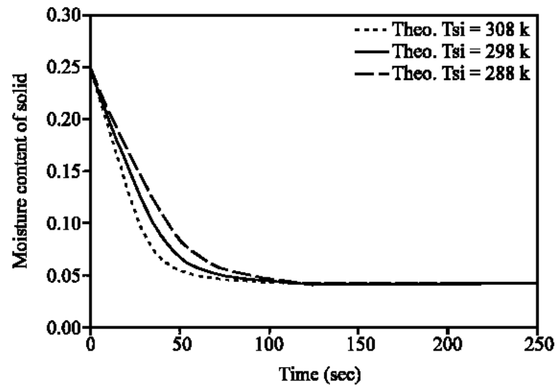

Fig. 6: Moisture content of solid in fluidized bed at various initial solid temperatures (288, 298 and 308 K)

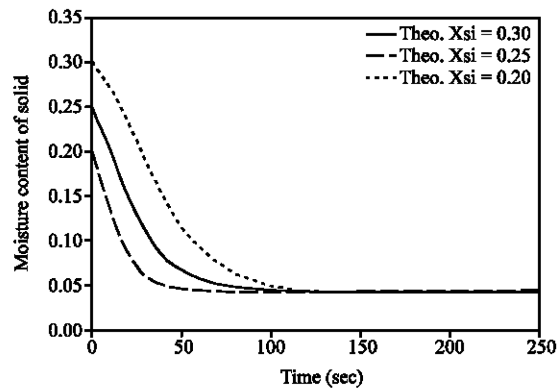

Fig. 7: Moisture content of solid in fluidized bed at various initial moisture contents of solid (0.2, 0.25 and 0.3)

parameters have no significant effect on dryer performance. The higher air velocity at a constant temperature can make the drying time, shorter. Figure 3 and 4 show temperature and moisture content profiles at two air temperatures (343 and 373 K) and constant gas velocity (4 m sec^{-1}).

As shown in Fig. 3 and 4, drying process with a low gas temperature reaches steady state condition faster than the higher gas temperature. The moisture content is at a high gas temperature is low. So, it causes a faster drying process. Further, two distinct zones in drying process are observed in these figures. At the first part the solids temperature increased versus time up to the saturation temperature. This temperature approximately is 367 K at higher gas temperature (373 K) and 340 K at lower gas temperature (343 K).

At the first part, moisture content of solids (drying rate) decreased versus time up to the final moisture content which was around 0.049 kg kg^{-1} at higher gas temperature and 0.08 kg kg^{-1} at lower gas temperature.

At the second part, the steady state condition and the particle temperature was equal to the saturation temperature and moisture content of solid was constant.

As shown in Fig. 3 and 4, there is a good agreement between theoretical data obtained from this work and the experimental data obtained from the literature however there are some deviations between those data (theoretical and experimental) related to the moisture contents.

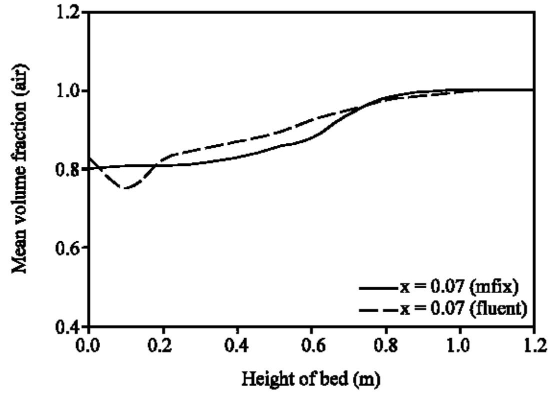

Fig. 8: Mean volume fraction of air in the bed (near wall (at x = 0.07 m))

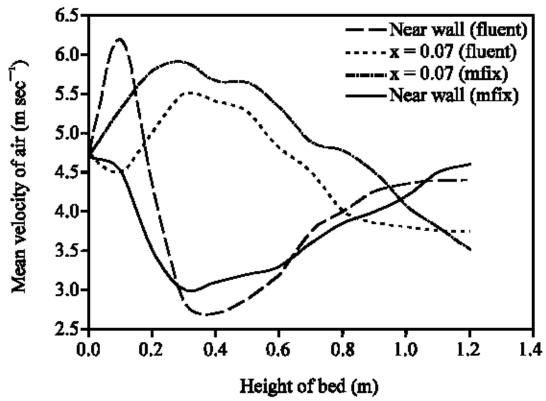

Fig. 9: Mean axial of air at two locations along the bed width (near wall (at x = 0.07 m))

The particle size effect on moisture content of solid has been shown in Fig. 5. As the particle diameter was decreased versus time, the drying rate was increased. The moisture content sharply reached equilibrium condition at smaller particles (d_p = 1 mm).

Figure 6 and 7 show the effect of the inlet moisture content and inlet temperature of the solid particles on the moisture content of solid. The inlet moisture content of particles had a significant effect on the dryer performance but the inlet temperature of the particles had no effect on it. Therefore, the fluidized bed dryer is more sensitive to the inlet gas temperature, initial solid moisture and particles size.

Figure 8 shows mean volume fraction of air along the bed height (on dryer wall while its radius is around 0.07 m). It shows an enhancement from the inlet zone to the outlet zone of bed.

Figure 9 shows mean axial air velocity at two locations along the radius of bed (center and near the wall) and compared results from our modeling with modeling results from commercial CFD software (Fluent 6.3).

Figure 10 to 12 show the mean radial velocity of air at four locations (y = 0.1, 0.3, 0.6 and 1.1 m) along the axis. The velocity profiles show a good agreement between the data obtained from simulation results and results from the Fluent software however some deviations are observed near the inlet zone of the bed (at y = 0.1 m).

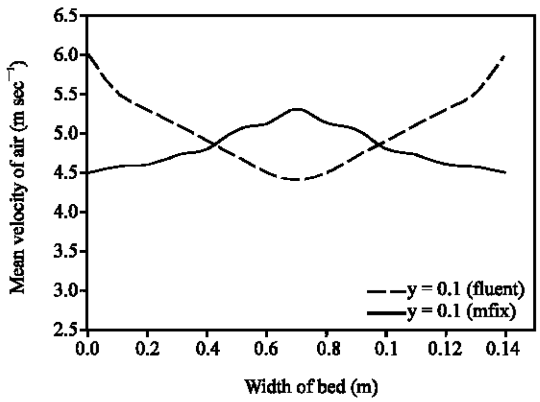

Fig. 10: Mean radial velocity of air at one location near the inlet zone of the bed (y = 0.1 m)

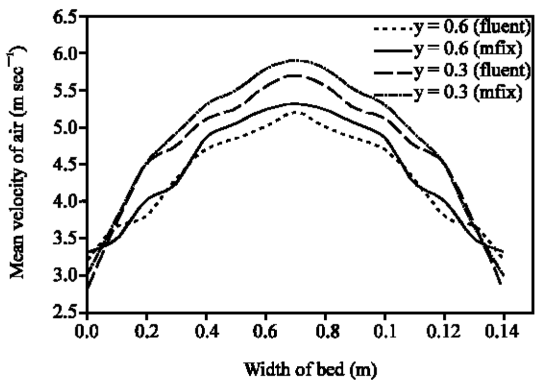

Fig. 11: Mean radial velocity of air at two locations in the middle zone of bed (y = 0.3 and 0.6 m)

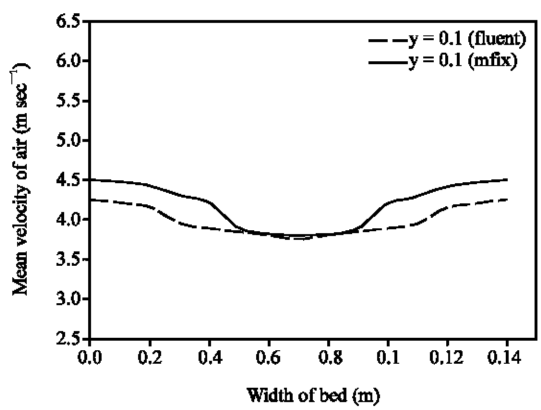

Fig. 12: Mean radial velocity of air at one location near the outlet zone of the bed (y = 1.1 m)

Figure 9 to 12 show when the air passes through the bed, near the inlet zone (at y = 0.1 m) and in the middle of the bed height (at y = 0.3, 0.6 m), mean air velocity is minimum near the wall bed (x = 0) and is maximum in the middle of the bed width (x = 0.07). Mean air velocity of the outlet zone of the bed (at y = 1.1 m) is maximum near the walls and decreases in the middle of the bed width. The maximum amount of air velocity is around the radial center of the bed (at y = 0.3 m).

CONCLUSIONS

A two fluid Eulerian model was used for modeling the heat and mass transfer in a fluidized bed dryer including wet wheat grains. The modeling was used to predict moisture and temperature distributions of solid at various drying times. The drying curve showed constant and decreasing rates. The operating conditions effects such as inlet gas velocity, inlet gas temperature, inlet solid temperature, initial solid moisture and particles size on the drying process were investigated. The modeling results showed a good agreement between the calculated data and the reported data in the literature.

NOMENCLATURE

a = Specific surface (1/m)
c = Specific surface kJ kg^{-1} °C
C_{DZ} = Two phase grag coefficient
d = Particle diameter (m)
D = Molecular diffusion (m^{-2} sec^{-1})
g = Gracity (m sec^{-2})
G (ε_g) = Solid stress modulus
h_v = Heat transfer dimensionless
k = Thermal conductivity (kJ kg^{-1} °C)
$\dot{m}$ = Moisture evaporation
Pr = Prandtl No.
P = Pressure (kPa)
Re = Reynolds number, as defined in text
r = Radial distance from the centerline (m)
T = Temperature (°C)
t = Time (sec)
u = Radial velocity (m sce^{-1})
v = Axial velocity (m sce^{-1})
x = Moisture content (kg_w/kg_s)
z = Elevation (m)

Greek symbols:

β = Gas-solid drag coefficient
γ_0 = Heat of vaporization (kJ kg^{-1})
ε = Void fraction
μ = Viscosity (kg $msec^{-1}$)
ρ = Density (kg m^{-3})
σ = Evaporation coefficient (kg m^{-2} sec)
τ = Stress (kPa)

Subscripts:

Dz = Grag in z-direction
g = Gas
p = Particle
pg = Gas on the surface of a particle

r = Radial
rr = Radial-stress
s = Solid
sz = Solid-axial
v = Vapor
z = Axial
zz = Axial-stress

REFERENCES

Azizi, S., S.H. Hosseini, G. Ahmadi and M. Moraveji, 2010. Numerical simulation of particle segregation in bubbling gas-fluidized beds. Chem. Eng. Technol., 33: 421-432.

Basirat-Tabrizi, H., M. Saffar-Avval and M.R. Assarie, 1983. Two dimensional mathematical modeling of fluidized bed drying. Proceedings of 2nd Trabzon International Energy and Environment Symposium, April 20-22, Begell House Inc., Trabzon, Turkey, pp: 363-363.

Basirat-Tabrizi, H., M. Saffar-Avval and M.R. Assarie, 2002. Two-dimensional mathematical model of a packed bed dryer and experimentation. Proc. Inst. Mechanical Eng. Part A J. Power Energy, 216: 161-168.

Burgschweiger, J. and E. Tsotsas, 2002. Experimental investigation and modelling of continuous fluidized bed drying under steady-state and dynamic conditions. Chem. Eng. Sci., 57: 5021-5038.

Chandran, A.N., S.S. Rao and Y.B.G. Varma, 1990. Fluidized bed drying of solids. AIChE J., 36: 29-38.

Ergun, S., 1952. Fluid flow through packed columns. Chem. Eng. Prog., 48: 89-94.

Garnavi, L., N. Kasiri and S.H. Hashemabadi, 2006. Mathematical modeling of a continuous fluidized bed dryer. Int. Commun. Heat Mass Transfer, 33: 666-675.

Gidaspow, D., 1994. Multiphase Flow and Fluidization: Continuum and Kinetic Theory Descriptions. Academic Press, Boston, MA, USA.

Groenewold, H. and E. Tsotsas, 1997. A new model for fluidized bed drying. Drying Technol., 15: 1687-1698.

Hajidavalloo, E. and F. Hamdullahpur, 2000a. Thermal analysis of a fluidized bed drying process for crops. Part I: Mathematical modeling. Int. J. Energy Res., 24: 791-807.

Hajidavalloo, E. and F. Hamdullahpur, 2000b. Thermal analysis of a fluidized bed drying process for crops. Part II: Experimental results and model verification. Int. J. Energy Res., 24: 809-820.

Hekmat, A., A.E. Amooghin and M.K. Moraveji, 2010. CFD simulation of gas-liquid flow behavior in an airlift reactor, determination of the optimum distance of the draft tube. Simulation Modeling Practice Theory, 18: 927-945.

Hoebink, J.H.B.J. and K. Rietema, 1980a. Drying granular solids in fluidized bed I. Description on basis of mass and heat transfer coefficients. Chem. Eng. Sci., 35: 2135-2139.

Hoebink, J.H.B.J. and K. Rietema, 1980b. Drying granular solids in fluidized bed II. The influence of diffusion limitation on the gas-solid contacting around bubbles. Chem. Eng. Sci., 35: 2257-2265.

Ishii, M., 1975. Thermo-Fluid Dynamic Theory of Two Phase Flow. Eyrelles Publisher, Paris, pp: 275.

Izadifar, M. and D. Mowla, 2003. Simulation of a cross-flow continuous fluidized bed dryer for paddy rice. J. Food Eng., 58: 325-329.

Kerkhof, P.J.A.M., 1994. Relations between local and effective air-side mass and heat transfer coefficients in fluidized bed rying. Drying Technol., 12: 1191-1210.

Lai, F.S. and Y. Chen, 1986. Modeling and simulation of a continuous fluidized bed dryer. Chem. Eng. Sci., 41: 2419-2430.

Mujumdar, A.S., 1995. Handbook of Industrial Drying. 2nd Edn., Marcel Dekker Inc., New York, USA.

Palancz, B., 1983. Mathematical model for continuous fluidized bed drying. Chem. Eng. Sci., 38: 1045-1059.

Souraki, B.A. and D. Mowla, 2008. Experimental and theoretical investigation of drying behavior of garlic in an inert medium fluidized bed assisted by microwave. J. Food Eng., 88: 438-449.

Souraki, B.A., A. Andre and D. Mowla, 2009. Mathematical modeling of microwave-assisted inert medium fluidized bed drying of cylindrical carrot samples. Chem. Eng. Process. Process Intensification, 48: 296-305.

Strumillo, C. and T. Kudra, 1996. Drying: Principles, Applications and Design. Gordon and Breach Science Publishers, New York, pp: 448.

Syahrul, S., F. Hamdullahpur and I. Dincer, 2002. Energy and Exergy Efficiencies of Fluidized Bed Drying of Moist Particles. In: Progress in Transport Phenomena, Dost, S., H. Struchtrup and I. Dincer (Eds.). Elsevier, USA., pp: 827-832.

Thomas, P.P. and Y.B.G. Varma, 1992. Fluidized bed drying of granular food materials. Powder Technol., 69: 213-222.

Tsotsas, E., 1994. From single particle to fluid bed drying kinetics. Drying Technol., 12: 1401-1426.

Van Ballegooijen, W.G.E., A.M. van Loon and A.J.J. van der Zanden, 1997. Modeling diffusion-limited drying behavior in a batch fluidized bed dryer. Drying Technol., 15: 837-855.

Vitor, J.F.A., E.C. Biscaia and G. Massarani, 2004. Modeling of biomass drying in fluidized bed. Proceedings of 14th International Drying Symposium, Aug. 22-25, Sao Paulo, Brazil, pp: 1104-1111.

Wang, Z.H. and G. Chen, 2000. Heat and mass transfer in batch fluidized-bed drying of porous particles. Chem. Eng. Sci., 55: 1857-1869.

Wildhagen, G.R.S., L.A. Calcada and G. Massarani, 2002. Drying of porous particles in fluidized beds: Modeling and experiments. J. Porous Media, 5: 123-133.

Zahed, A.H., J.X. Zhu and J.R. Grace, 1995. Modeling and simulation of batch and continuous fluidized-bed dryers. Drying Technol., 13: 1-28.